Biochimica et Biophysica Acta 1838 (2014) 2001–2010

Contents lists available at ScienceDirect

Biochimica et Biophysica Acta

journal homepage: www.elsevier.com/locate/bbamem

Elucidating the mechanisms of protein antigen adsorption to the CAF/NAF liposomal vaccine adjuvant systems: Effect of charge, fluidity and antigen-to-lipid ratio

Mette Hamborg [a,*,1], Fabrice Rose [a,1], Lene Jorgensen [a], Katrine Bjorklund [a], Helene B. Pedersen [a], Dennis Christensen [b], Camilla Foged [a,*]

[a] Department of Pharmacy, Faculty of Health and Medical Sciences, University of Copenhagen Universitetsparken 2, DK-2100 Copenhagen Ø, Denmark
[b] Department of Infectious Disease Immunology, Vaccine Delivery & Formulation, Statens Serum Institut, Artillerivej 5, DK-2300 Copenhagen S, Denmark

ARTICLE INFO

Article history:
Received 7 November 2013
Received in revised form 11 April 2014
Accepted 17 April 2014
Available online 25 April 2014

Keywords:
Liposome
Drug delivery
Adjuvant
Antigen adsorption
Subunit vaccine

ABSTRACT

The reverse vaccinology approach has recently resulted in the identification of promising protein antigens, which in combination with appropriate adjuvants can stimulate customized, protective immune responses. Although antigen adsorption to adjuvants influences vaccine efficacy and safety, little is generally known about how antigens and adjuvants interact at the molecular level. The aim of this study was to elucidate the mechanisms of interactions between the equally sized, but oppositely charged model protein antigens α-lactalbumin and lysozyme, and i) the clinically tested cationic liposomal adjuvant CAF01 composed of cationic dimethyldioctadecylammonium (DDA) bromide and trehalose-6,6′-dibehenate (TDB) or ii) the neutral adjuvant formulation NAF01, where DDA was replaced with zwitterionic distearoylphosphatidylcholine (DSPC). The effect of liposome charge, bilayer rigidity, isoelectric point and antigen-to-lipid ratio was investigated using dynamic light scattering, transmission electron microscopy, differential scanning calorimetry, intrinsic fluorescence and Langmuir monolayers. The net anionic α-lactalbumin adsorbed onto the cationic liposomes, while there was no measureable attractive interaction with the zwitterionic liposomes. In contrast, the net cationic lysozyme showed very little interaction with either types of liposome. Adsorption of α-lactalbumin altered its tertiary structure, affected lipid membrane packing below and above the phase transition temperature, and neutralized the liposomal surface charge, resulting in reduced colloidal stability and liposome aggregation. Langmuir studies revealed that α-lactalbumin was not squeezed out of DDA monolayers upon compression, which suggests additional hydrophobic interactions.

Such interactions are thus likely to affect the way vaccine antigens are presented to antigen-presenting cells, and may play an important role for the efficacy of the vaccine-induced immune response. These studies thus exemplify the importance of characterizing the molecular interactions between the vaccine antigen and adjuvant along with immunogenicity and efficacy studies.

© 2014 Elsevier B.V. All rights reserved.

1. Introduction

In recent years, the reverse vaccinology approach towards subunit vaccine design has resulted in the identification of a number of promising pathogen-derived recombinant protein antigens with significantly improved safety profiles, as compared to the live attenuated and whole inactivated pathogens that traditionally have been used as vaccines [1]. However, since highly purified protein-based antigens in general are weakly immunogenic by themselves, co-administration of appropriate adjuvants is required to potentiate the immune response [2]. Aluminum-based adjuvants have routinely been used in marketed human vaccines to stimulate long-lived protective immune responses, but their applicability is limited by the fact that they only induce antibody-mediated immune responses [3]. Stimulation of cell-mediated and/or mucosal immunity is though a prerequisite for preventing more difficult infectious diseases like tuberculosis, malaria and AIDS with vaccines [4]. A number of novel adjuvant systems that can induce such immune responses are therefore in clinical development [5].

A promising example is the cationic liposomal adjuvant CAF01 (Statens Serum Institut, Denmark), which is based on a binary mixture of the cationic surfactant dimethyldioctadecylammonium (DDA)

Abbreviations: Cryo-TEM, Cryo transmission electron microscopy; DDA, dimethyldioctadecylammonium bromide; DLS, dynamic light scattering; DSC, differential scanning calorimetry; DSPC, distearoylphosphatidylcholine; SOI, site of injection; TDB, trehalose-6,6′-dibehenate

* Corresponding authors. Tel.: + 45 35 33 64 02; fax: +45 35 33 60 01.
E-mail addresses: mette.hamborg@sund.ku.dk (M. Hamborg), camilla.foged@sund.ku.dk (C. Foged).

[1] These authors contributed equally.

http://dx.doi.org/10.1016/j.bbamem.2014.04.013
0005-2736/© 2014 Elsevier B.V. All rights reserved.

bromide and the immunopotentiator α,α′-trehalose 6,6′-dibehenate (TDB) [6]. This adjuvant has been tested in phase 1 clinical trials in combination with the tuberculosis fusion antigen Ag85B-ESAT6 (H1) (NCT ID: NCT00922363) and an HIV-1 peptide mix (NCT ID: NCT01141205; NCT01009762), respectively. These gel state DDA/TDB liposomes potentiate a strong $CD4^+$ T-cell response characterized by a mixed Th1/Th17 profile [7–9]. Their adjuvant properties are highly dependent on their physicochemical properties like surface charge, size and membrane rigidity, which are decisive for the adjuvant mechanism(s) and thus the vaccine efficacy and safety [10–12]. Studies have thus shown that co-administration of antigens with such cationic liposomes leads to the induction of stronger and qualitatively different antigen-specific immune responses than co-administration with neutral or anionic liposomes of similar thermotropic phase behavior [13,14]. In addition, the gel state of the liposomes is apparently a prerequisite for their adjuvant activity, because replacement of the DDA component with unsaturated or shorter-chain analog abolishes their adjuvant activity [10]. Compared to neutral/anionic liposomes with similar thermotropic phase behavior, the CAF01 adjuvant has distinct advantages since it mediates the avid binding and retention of the antigen(s) at the site of injection (SOI) and enhances immunogenicity, eventually resulting in strong cell-mediated immune responses [7,11]. However, a prerequisite for the strong adjuvant effect of CAF01 is that the antigen is co-localized with the immunopotentiator, either through encapsulation or by strong surface adsorption: Kamath et al. showed that administration of free antigen (TB vaccine candidate H1) one day before or simultaneous to vaccination with the vaccine containing H1 complexed to CAF01 reduced the ability of the vaccine to induce a CMI response. This was related to the presence of high amounts of dendritic cells exposed only to the antigen, which due to lack of co-stimulation by the adjuvant would create temporary anergy to activation of antigen-specific T-cells [8]. It is thus pivotal to understand interactions at the molecular level between vaccine candidates and adjuvants in order to ensure optimal vaccine efficacy.

Electrostatic interactions are generally considered to be the main driving forces for surface adsorption of protein antigens onto cationic liposomes [11,15,16]. However, little is generally known about how antigens and adjuvants interact at the molecular level. This is primarily because the application of most analytical methods for characterization of antigen-adjuvant mixtures is limited by i) the structural complexity of protein antigens and adjuvants, ii) the particulate nature of most adjuvants and iii) the relatively low protein antigen doses required for efficacy [17]. Interactions between liposomes and proteins can be measured by using a range of analytical methods; indirect measurements include for example an assessment of the colloidal stability, the permeability of the liposomal membrane and the structural changes of the proteins upon adsorption, or direct measurements including e.g. single molecule techniques, isothermal titration calorimetry (ITC) and monolayer techniques.

In the present study, we performed systematic adsorption studies by investigating the two equally sized, but oppositely charged highly pure and well-characterized model proteins α-lactalbumin and lysozyme (Table 1) and the cationic liposomal adjuvant CAF01 or the neutral adjuvant formulation NAF01, in which DDA has been replaced with zwitterionic distearoylphosphatidylcholine (DSPC). The aim was to elucidate their mechanisms of interaction via biophysical investigations by applying a number of different analytical methods. These included dynamic light scattering (DLS) and cryo-transmission electron microscopy (cryo-TEM). Subsequently, the effect of the interactions on the membrane thermotropic phase behavior as well as the protein structure was investigated by applying differential scanning calorimetry (DSC) and intrinsic fluorescence, respectively. Finally, the molecular interactions were studied further by using the Langmuir monolayer technique.

2. Materials and methods

2.1. Materials

DDA and DSPC were obtained from Avanti Polar Lipids (Alabaster, AL, USA). TDB was synthesized by Clausen-Kaas A/S (Farum, Denmark). The model proteins were obtained from Sigma-Aldrich (St. Louis, MO, USA); α-lactalbumin (L5385, ≥85%), α-lactalbumin Ca^{2+} depleted (L6010, ≥85%), and lysozyme (L6876, >90%). MeOH and $CHCl_3$ (extra pure) were purchased from VWR (Leuven, Belgium) and Merck (Darmstadt, Germany), respectively. Purified Milli-Q water was used for all buffers. The protein stock solutions were prepared in 10 mM Tris buffer (pH 7.4), and their concentrations were determined by UV spectroscopy at 280 nm by using a NanoDrop spectrophotometer (Thermo scientific, Wilmington, DE, USA) applying published extinction coefficients.

2.2. Preparation of liposomes by the thin film method

The liposomes were prepared by the thin film method essentially as described previously [6], but with a few modifications. Briefly, weighed amounts of DDA, TDB and DSPC were dissolved in $CHCl_3$–MeOH (9:1, v/v) and aliquots from these stocks were mixed in a 50 mL round-bottomed flask resulting in lipid mixtures of different molar ratios (Table 2). The total lipid content per batch was 22.34 μmol. The organic solvent was evaporated under vacuum resulting in the formation of thin lipid films. The films were stripped twice with EtOH and dried overnight to remove trace amounts of the organic solvents. The lipid films were rehydrated with Tris buffer (10 mM, pH 7.4) and sonicated for 5 min using a Branson 2510 Ultrasonic Cleaner (Danburry, CT, USA), followed by heating at 80 °C in a water bath. Every 10 min, the dispersions were whirl-mixed vigorously by using a VELP Scientifica wizard vortex mixer (Usmate, Milano, Italy) combined with tip-sonication for 20–120 s by applying a 150 W Branson tip-sonicator (85-% of the duty cycle) to reduce the size and to avoid size reduction by e.g. extrusion that causes an unnecessary loss of lipid during processing.

The average liposome size distribution and polydispersity index (PDI) were analyzed by DLS by using the photon correlation spectroscopy technique. The surface charge of the particles was estimated by analysis of the zeta potential (laser-Doppler electrophoresis). For the size measurements, the samples were diluted 10 times, whereas for the zeta potential measurements, the samples were diluted 300 times in 10 mM Tris buffer to a lipid concentration of approximately 14.9 μM. The measurements were performed at 25 °C by using a Zetasizer Nano ZS (Malvern Instruments, Worcestershire, UK) equipped with a 633 nm laser and 173° detection optics. For viscosity and refractive index, the values of pure water were used. Malvern DTS v.6.20 software was used for data acquisition and analysis. A Nanosphere™ Size

Table 1
Physicochemical characteristics of α-lactalbumin and lysozyme [18–21].

Protein	Dimensions (nm)	M_w (Da)	pI	Net charge at pH 7.0	Hydrophobicity (Cal/residue)[a]	Surface hydrophobicity[b]
α-Lactalbumin	2.3 × 2.6 × 4.0	14,175	5.5[c]	−5.3[c]	1150	1.66
Lysozyme	4.5 × 3.0 × 3.0	14,300	11.1[c]	8.4[c]	970	7.49

[a] Calculated from the amino acid sequence.
[b] Determined as the retention coefficients from hydrophobic column chromatography.
[c] Calculated from PROPKA 3.1 from PDB file (2LYZ.pdb/1F6S.pdb).

Table 2
The composition, size, polydispersity index and zeta potential of the liposomal formulations. The results denote mean ± SD (n = 3).

DDA/TDB/DSPC molar ratio	Size (*nm*)	PDI	Zeta potential (*mV*)
(89:11:0, CAF01)	168 ± 1	0.25 ± 0.01	66.7 ± 5.3
(67:11:22)	141 ± 7	0.26 ± 0.03	55.0 ± 3.9
(22:11:67)	141 ± 9	0.26 ± 0.03	48.6 ± 2.1
(0:11:89, NAF01)	176 ± 51	0.55 ± 0.17	−5.2 ± 3.7

Standard (220 ± 6 nm, Duke Scientific Corporation, Palo Alto, CA, USA) and a zeta potential transfer standard (−50 ± 5 mV, Malvern Instruments) were used to verify the performance of the instrument. The particle size distribution was reflected in the PDI, which ranges from 0 for a monodisperse to 1.0 for an entirely heterodisperse dispersion.

2.3. Protein influence on the liposome size and the zeta potential

Equal volumes of liposome dispersions and protein solutions were mixed and left to equilibrate for at least 10 min prior to the size and zeta potential measurements, which were performed as described above. Below a protein-to-lipid weight ratio of 0.44, the lipid concentration was kept constant at 2.2 mM, whereas the protein concentration was varied systematically. Above a protein-to-lipid weight ratio of 0.44, the protein concentration was kept constant and the liposome dispersions were diluted in two-fold steps.

2.4. Cryo-TEM

Morphological analysis was carried out by using cryo-TEM applying a Philips CM120 BioTWIN transmission electron microscope (Philips, Eindhoven, the Netherlands). The samples for the cryo-TEM were prepared under controlled temperature and humidity conditions within an environmental verification system. A small droplet (5 μL) of sample was deposited onto a Pelco Lacey carbon-filmed grid. The droplet was spread carefully, and excess liquid was removed with a filter paper, resulting in the formation of a thin (10–500 nm) sample film. Then, the samples were immediately plunged into liquid ethane at −180 °C. The vitrified samples were subsequently transferred in liquid nitrogen to an Oxford CT3500 cryo holder connected to the electron microscope. The sample temperature was continuously kept below −180 °C. All observations were made in the bright field mode at an acceleration voltage of 120 kV. Digital pictures were recorded with a Gatan Imaging Filter 100 CCD camera (Gatan, Pleasanton, CA, USA).

2.5. Intrinsic fluorescence spectroscopy

Intrinsic fluorescence spectra were acquired by using a Spex Fluorolog 3-22 (HORIBA Jobin Yvon SAS, Longjumeau Cedex, France) equipped with a 450-W Xenon lamp. An excitation wavelength of 295 nm (>95% Trp emission) was used, and the emission spectra were collected from 305 to 405 nm (slit widths of 2 nm and 4 nm, respectively) at a 1 nm/s data collection rate and a 1 s integration time. All spectra were background-corrected by subtracting the corresponding buffer or liposome spectrum. The final protein concentration was 14.1 μM and the final lipid concentration was 0.2 mM.

2.6. Differential scanning calorimetry

The thermal stability of the model proteins and the gel-to-liquid crystalline phase transition temperature (T_m) of the vesicles in suspension were determined by using DSC. Equal volumes of liposome dispersions and protein solutions in 10 mM Tris buffer pH 7.4 were mixed. The final lipid concentrations were approximately 2.2 mM. The final protein concentrations were in the range of 7.1–529.1 μM for α-lactalbumin and in the range of 7.0–524.5 μM for lysozyme. All samples and buffer were degassed for approximately 10 min prior to the measurements. Data collection was performed by using a Nano DSC (TA instruments, New Castle, DE, USA) at a scanning rate of 0.5 °C/min in the temperature range of 20 °C to 60 °C for the DDA liposomes, and from 20 °C to 75 °C for the DSPC-containing liposomes. Thermograms for the pure protein samples were recorded at a scanning rate of 1 °C/min in the temperature range from 20 °C to 110 °C (Supplementary information). The reversibility of the thermotropic phase behavior of the liposomes mixed with the proteins was examined by performing a second heating scan after cooling down to 20 °C. A buffer scan recorded from 20 °C to 85 °C applying a scanning rate of 2 °C/min was performed between scans of different liposome batches and proteins to ensure a sufficient cleaning of the sample cell. The NanoAnalyze Data Analysis program version 2.2.0 (TA Instruments) was used to subtract the curve for the second buffer scan from each individual sample scan. The Origin® 7 SR2 scientific plotting software (OriginLab Corporation, Northhampton, MA, USA) was used for baseline correction and data analysis. The T_{max} is the temperature at which the excess heat capacity, C_p, is at its maximum. The change in enthalpy (ΔH) was determined by integrating the area under the baseline-corrected C_p curve obtained for each sample.

2.7. Langmuir monolayers

To address the effect of the differently charged head groups on the interactions with the antigens the monolayer model was simplified in such a manner that it only comprised DDA or DSPC (without TDB). A previous study has shown that the collapse of DDA monolayers occurs at similar surface pressure and mean molecular area as the collapse of DDA/TDB monolayers, which also justifies to leave out TDB from the studies [22]. The surface pressures were measured for the lipid monolayers alone and in the presence of 4.5 nmol protein, which was added to the subphase before spreading of the DDA or DSPC (27.7 nmol in chloroform) by using a Hamilton syringe. The experiments were performed by using a KSV Minitrough 1 (KSV Instruments Ltd., Helsinki, Finland) with a surface area of 24,300 mm^2. The surface pressure was measured by using a platinum Wilhelmy plate. All experiments were performed on a 175 mL subphase consisting of 10 mM Tris buffer (pH 7.4) kept at 22 °C by means of tempered water circulating underneath the Langmuir trough. The surface pressure was pre-set to zero before spreading of the DDA or DSPC. For the lipid monolayers investigated in the absence of protein, the compression was initiated 10 min after spreading to allow for the complete evaporation of the chloroform. For experiments with protein present in the subphase, the compression was initiated 20 min after spreading the lipids to allow for evaporation of the chloroform and for the equilibration of the proteins. The monolayers were compressed at a constant rate of 10 mm/min. Data analysis was performed by using the KSV software (KSV Instruments Ltd.). For monolayers consisting of protein only, the degree of compression was described as the surface pressure as a function of the mean protein molecular area, whereas for the lipid-containing monolayers, the degree of compression was described as the surface pressure as a function of the mean lipid molecular area. The phase transitions and the collapse points were estimated from the compression modulus (Cs^{-1}) versus Π dependency, where Cs^{-1} is defined according to Eq. (1):

$$Cs^{-1} = -A(d\Pi/dA). \quad (1)$$

A characteristic minimum for the C_S^{-1} versus Π dependency for the monolayer reflects the phase transition from the liquid-expanded to the liquid-condensed states of the monolayer, whereas the surface pressure at $(d\Pi / dA) = 0$ identifies the monolayer collapse.

2.8. Statistics

Statistical calculations were performed by using GraphPad Prism 6 (GraphPad Software, Inc., La Jolla, CA, USA) by a one-way analysis of variance at a 0.05 significance level followed by means comparison by applying the Tukey's test.

3. Results

3.1. Choice of model proteins and experimental conditions

To study the mechanisms of protein–liposome interactions and in particular the effect of charge, α-lactalbumin and lysozyme were chosen as model proteins since they have different isoelectric points; lysozyme is positively charged at pH 7.4, whereas α-lactalbumin is negatively charged (Table 1), but they are otherwise highly homologous and share similar primary, secondary and tertiary structures [23–25]. In addition, they are small, relatively simple, well-characterized, readily available and highly pure proteins, which make them ideal for the present biophysical studies. Both proteins are single domain proteins that are cross-linked via four disulfide bridges [23]. The tertiary structure of the native α-lactalbumin is in addition stabilized by Ca^{2+} bound at the specific Ca^{2+}-binding site [25,26]. The depletion of Ca^{2+} is manifested by a loss of tertiary structure and an increased surface hydrophobicity, eventually resulting in the Ca^{2+}-depleted α-lactalbumin structure being more expanded and flexible, as compared to the native Ca^{2+}-binding protein [27]. The increased flexibility of the Ca^{2+}-depleted molecule has been suggested to be the cause of its enhanced interaction with membranes, as compared to the native protein [28]. All the experiments were performed in 10 mM Tris buffer, pH 7.4, because the CAF01 adjuvant has an optimal stability in this buffer, which is also applied for the CAF01 formulation used in the clinical studies.

3.2. Physicochemical characteristics of CAF01 and NAF01

To study the effect of electrostatic interactions, the cationic DDA component of CAF01 was replaced in a step-wise manner with the zwitterionic (neutral) DSPC, which has the same acyl chain length (18 carbons) as the DDA alkyl chain. This resulted in systematically varied lipid molar ratios with liposomes containing 0, 22, 67 and 89 mol-% DSPC, respectively, at a constant TDB molar ratio (11 mol%, Table 2). The DSPC component was selected because it has a main gel-to-liquid phase transition temperature above 37 °C (actual value 55 °C) like DDA (actual value 47 °C). Hence, both the cationic DDA/TDB liposomes (CAF01) and the zwitterionic DSPC/TDB liposomes (NAF01) are in their gel state at 25 °C as well as 37 °C. Exchanging the cationic DDA with the zwitterionic DSPC reduced, as expected, the zeta potential of the liposomes from approximately 66.7 mV to −5.2 mV (Table 2). Replacing a molar fraction of DDA with DSPC (25% and 75%, respectively) resulted in a slight reduction of the average particle size from 168 nm to 141 nm. The DSPC/TDB liposomes were less physically stable, as compared to the DDA-containing liposomes (data not shown). Thus, the experiments with DSPC/TDB liposomes were conducted within 24 h of their preparation.

3.3. Attractive electrostatic interactions with α-lactalbumin cause aggregation of the cationic liposomes

The interactions between the liposomes and the proteins were studied by characterizing the colloidal behavior of the liposome dispersions upon protein adsorption. The results clearly confirmed that CAF01 interacted strongly with α-lactalbumin (Fig. 1A). Adsorption of the slightly net negatively charged α-lactalbumin to CAF01 resulted in a decreased zeta potential, which was accompanied by an increased liposome size due to the reduced colloidal stability. The average liposome sizes presented in Fig. 1A are above the size detection limit of the

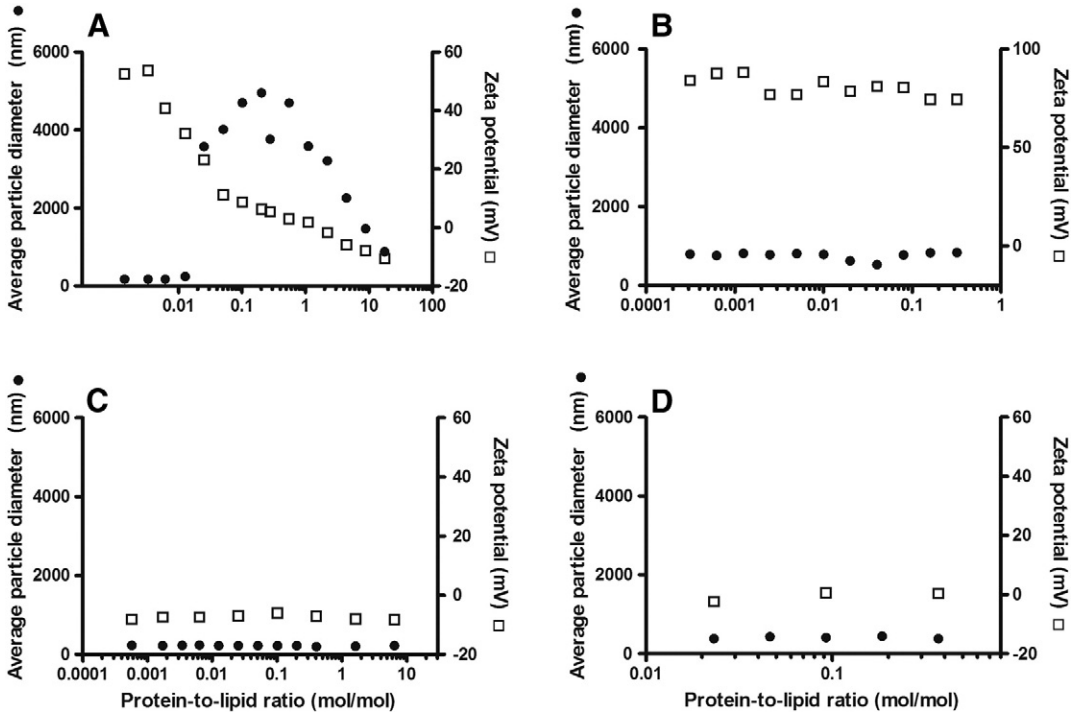

Fig. 1. Representative size and zeta potential of CAF01 (A and B) and NAF01 (C and D) (2.2 mM) upon addition of different concentrations of α-lactalbumin (A and C) and lysozyme (B and D). The diameters shown on the y-axis are scattering intensity-based (Z-ave). Large aggregates outside the measurement range of the instrument were observed in the molar ratio range of 0.022 to 18 (A).

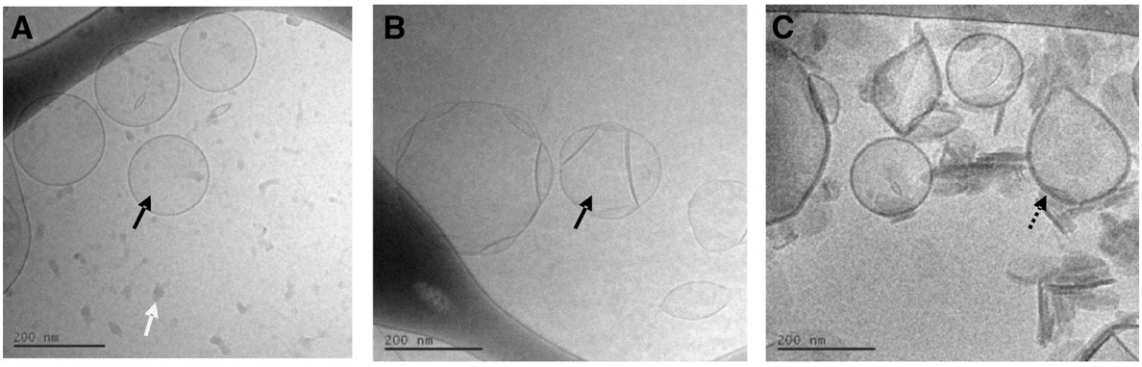

Fig. 2. Cryo-TEM micrographs of CAF01 upon addition of A) lysozyme at a protein-to-lipid molar ratio of 0.03, B) α-lactalbumin at a protein-to-lipid molar ratio of 0.003 and C) α-lactalbumin at a protein-to-lipid molar ratio of 0.24. Black, solid arrows (A and B): Liposomes; Black, round dot arrow (C): Protein layer on the liposome surface; White arrow (A): Frost. Scale bars: 200 nm.

method (1 μm) and should therefore only be taken as rough estimates reflecting the general stability (or instability) of the liposome dispersion after protein addition. Liposome aggregation was caused by α-lactalbumin at protein-to-lipid molar ratios of 0.02 to 18. This range is rather broad, as compared to previous studies with bovine serum albumin (BSA) and ovalbumin, suggesting that the protein-accessible lipid surface area increases as a function of the α-lactalbumin concentration, or that the adsorbed protein layer (corona) is not capable of or sufficient for stabilizing the liposomes [17]. In contrast, there was no measurable attractive interaction with the net positively charged lysozyme and CAF01 (Fig. 1B). Additionally, neither α-lactalbumin nor lysozyme affected the size and zeta potential of NAF01 suggesting that no attractive interactions exist between the proteins and the liposomes (Fig. 1C and D).

The cryo-TEM pictures were used to verify that the morphology of the cationic liposomes was preserved in the presence of lysozyme (Fig. 2A), while α-lactalbumin indeed caused aggregation of the liposomes and altered their morphology and membrane appearance (Fig. 2B and C). At a protein-to-lipid molar ratio of 0.24, the α-lactalbumin-coated liposomes formed larger clusters co-existing with more elongated lipid structures (Fig. 2C). The presence of the proteins on the membrane surface of the liposome was clearly visible as an increased bilayer thickness (approximately 12 nm, as compared to a normal bilayer thickness of 4–5 nm). To estimate if the increase in membrane thickness reflects the existence of a protein monolayer or a different adsorption pattern is beyond the resolution limit of the cryo-TEM technique (4–5 nm). However, at the lowest protein-to-lipid molar ratio under study (0.003, Fig. 2B), dispersed liposomes were observed, although they appeared more multivesicular than the control.

3.4. Adsorption to CAF01 alters the tertiary structure of α-lactalbumin

From the size measurements presented above, it is evident that α-lactalbumin adsorbs onto CAF01. It was therefore investigated if the tertiary structure of α-lactalbumin was altered upon adsorption by using intrinsic fluorescence, which is applied to measure the polarity of the Trp environment of the protein. For the native protein, two of the five Trp residues are solvent-exposed, while three are buried in the hydrophobic interior [29].

The calcium-saturated α-lactalbumin (the holo-form) in buffer showed a peak position at 334 nm, suggesting that the Trp residues on average are buried (Fig. 3 and Table 3). Upon adsorption to CAF01, a significant red shift of 14 nm was observed (from 334 nm to 348 nm), while the peak position was unchanged in the presence of NAF01. The intrinsic fluorescence of Ca^{2+}-depleted α-lactalbumin was measured for control purposes. The depleted form showed a peak position at 349 nm, which was unaffected by the addition of CAF01 and NAF01. The red shift of calcium-saturated α-lactalbumin observed upon adsorption to CAF01 indicates that the Trp groups of the adsorbed α-lactalbumin appear to exist in a more aqueous environment similar to the depleted α-lactalbumin (the apo-form). A decrease in the fluorescence signal was expected due to the light scattering caused by the liposomes, and this was observed for the NAF01 but not for CAF01, which increased the fluorescence intensity.

3.5. α-Lactalbumin interacts strongly with the cationic domains of the liposomes and alters their thermotropic phase behavior

The consequences of protein interaction on the thermotropic phase behavior of the liposomes were studied further by using DSC. Dispersions of DDA have previously been reported to have one sharp phase transition around 46.7 °C [22]. The thermogram for CAF01, representing the gel-to-liquid phase transition, consisted of two or

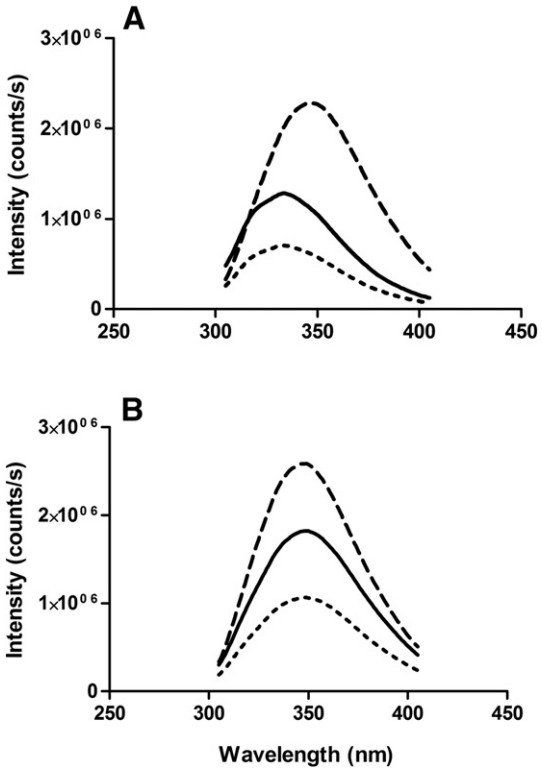

Fig. 3. Intrinsic fluorescence of A) Ca^{2+}-containing α-lactalbumin alone (solid), with CAF01 (dash) and with NAF01 (dot) as well as B) Ca^{2+}-depleted α-lactalbumin alone in the apo state (solid), with CAF01 (dash) and with NAF01 (dot). The final protein concentration was 14.1 μM and the final lipid concentration was 0.22 mM.

Table 3
The peak position of the Trp emission spectra. The results denote mean ± SD (n = 3).

	Peak position (nm)
α-Lactalbumin (Ca^{2+})	333.7 ± 0.6
α-Lactalbumin (Ca^{2+}) + CAF01	348.0 ± 1.0***
α-Lactalbumin (Ca^{2+}) + NAF01	333.3 ± 0.6
α-Lactalbumin (Ca^{2+}depleted)	349.0 ± 0.0***
α-Lactalbumin (Ca^{2+}depleted) + CAF01	348.7 ± 0.6***
α-Lactalbumin (Ca^{2+}depleted) + NAF01	348.7 ± 0.6***

*** $p < 0.001$, as compared to α-lactalbumin (Ca^{2+}).

more interconnected peaks between approximately 42 °C and 47 °C (Fig. 4A). This suggests that the two lipid components (DDA and TDB) are inhomogeneously distributed, resulting in the existence of microdomains enriched in one of the two components of different phase transitions, as reported previously [6]. A certain batch-to-batch variation in the appearance of the peaks was observed, probably caused by slight differences in the mixing procedure (data not shown). The thermogram for NAF01 showed a sharp peak with a T_m of 53 °C (Fig. 4B). Moreover, the thermotropic phase behavior of both types of liposomes was reversible, since the first and the second scans were identical (results not shown).

Addition of α-lactalbumin had a pronounced effect on the appearance of the phase transition of CAF01; addition of α-lactalbumin (70.5 μM) resulted in a decreased average Tm and increased ΔH (Fig. 4A and Supplementary information). In addition after the second heating, the transition was narrowed from three interconnected peaks to one peak suggesting a more orchestrated transition (Fig. 4B). Also, α-lactalbumin had a minor effect on NAF01. Lysozyme did not influence the thermotropic phase behavior of neither CAF01 nor NAF01 (data not shown).

An interesting phase separation phenomenon was observed for the liposomes consisting of ternary mixtures of DDA, TDB and DSPC (67:11:22, Fig. 5). The phase transition peak was very broad, which indicates that the lipid components are inhomogeneously distributed in the membrane. However, addition of 70.5 μM α-lactalbumin resulted in two distinct phase transitions with broad peaks around 42 °C and 55 °C, respectively, suggesting a complete separation of the DDA and DSPC domains (Fig. 5). Upon the second heating, the first of the two peaks, which is dominated by DDA (shown in Fig. 4) disappeared. This indicates that the reversibility between the gel state and the liquid state of the DDA-enriched domains has been lost. It is hypothesized that α-lactalbumin interacts mainly with the alkyl chains of DDA and not with the acyl chains of DSPC since the reversible nature of the phase transition temperature of 55 °C (mainly DSPC, Fig. 4b) was maintained during the heating process.

3.6. Hydrophobic interactions are evident from Langmuir isotherms

The Langmuir monolayer technique was subsequently applied to study the nature of the interactions further at the molecular level.

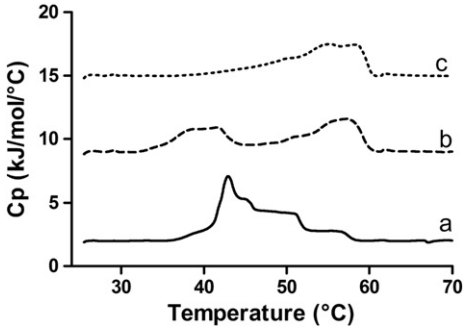

Fig. 5. Thermograms of 2.2 mM mixed DDA/TDB/DSPC liposomes at a molar ratio of 67:11:22 a) alone, b) mixed with 70.5 μM α-lactalbumin (first scan) and c) with 1 mg/mL α-lactalbumin (second scan).

Monolayer techniques, such as the Langmuir technique, have been widely applied to gain mechanistic information about how proteins affect the interfacial properties and packing of lipid monolayers [30,31]. Although a lipid monolayer at the air–water interface clearly deviates from lipid bilayer vesicles, it has been widely accepted as a useful model to study interactions with lipid bilayers [32]. The values for the surface pressure (Π) and the mean molecular area (A) at the minimum compression, at the monolayer collapse and at the phase transition from the liquid-expanded to the liquid-condensed phase are listed in Tables 4 and 5. Pure DDA and DSPC monolayers collapsed at a surface pressure of 46.4 mN/m and 60.9 mN/m, and with a mean molecular area of 45.6 $Å^2$ and 42.2 $Å^2$, respectively (Fig. 6A and B), as shown in previous studies [22,33]. Compression of the DDA monolayer resulted in a phase transition from the liquid-expanded to the liquid-condensed state at 13.4 mN/m and at an area of 72.6 $Å^2$ (Fig. 6A), while the DSPC monolayer compression showed a typical condensed isotherm (Fig. 6B).

The contribution of the proteins to the surface pressure was determined by adding the respective proteins to the subphase and equilibrating for 20 min before initiating the compression in the absence of the lipids. The Langmuir isotherms for the pure proteins (4.5 nmol) showed similar surface activities for α-lactalbumin and lysozyme (Supporting information), and their compression isotherms were incomplete, as observed previously at low protein concentrations [34]. Given this, it is most likely the lipids that provide the main contribution to the surface pressure when the lipids are spread on protein-containing subphases. When calculating the mean molecular area at the interface, only the lipid contribution was thus taken into account and not the protein contribution due to the difficulty in quantifying the amount of protein present at the interface. The lipids were spread onto the protein-containing sub phase, and the system was equilibrated for 20 min prior to initiating the compression. The addition of α-lactalbumin to the subphase resulted in an increase of the initial surface pressure of the DDA monolayer from 0.6 to 2.1 mN/m due to the accumulation of the protein at the interface (Table 4). In contrast, lysozyme appeared not to contribute to the initial surface pressure. The presence

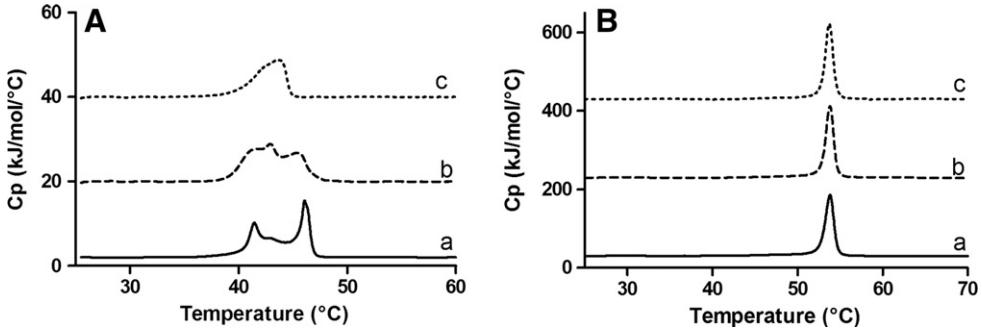

Fig. 4. Thermograms of CAF01 (2.2 mM) (A) and NAF01 (2.2 mM) (B) mixed with α-lactalbumin. The thermograms represent liposomes a) alone, b) with 70.5 μM protein (first scan) and c) with 70.5 μM protein (second scan).

Table 4
The surface pressure of DDA monolayers at minimum compression, at the collapse point and at the phase transitions, the two latter are also described by the mean molecular area. The results denote mean ± SD (n = 3).

	Minimum compression	Collapse point		Phase transition	
	mN/m	*mN/m*	*Å²*	*mN/m*	*Å²*
DDA	0.5 ± 0.1	46.4 ± 1.1	46.0 ± 1.3	13.4 ± 0.7	72.6 ± 1.4
DDA + α-lactalbumin	2.1 ± 0.0***	47.0 ± 1.7	44.8 ± 1.4*	13.4 ± 1.1	95.8 ± 0.6***
				30.6 ± 1.8***	60.4 ± 0.2***
DDA + lysozyme	1.0 ± 0.4	45.4 ± 1.7	48.9 ± 1.4	13.8 ± 1.3	84.0 ± 2.1***

* $p < 0.05$, as compared to DDA + lysozyme.
*** $p < 0.001$, as compared to DDA.

of α-lactalbumin resulted in a more expanded DDA isotherm, evident from a shift towards a higher surface pressure and an apparently larger area per lipid molecule (Fig. 6A). The protein affected the packing of the lipid monolayer, probably by imposing a deformation or a tilt effect on the lipid monolayer, as described previously in the literature [35,36]. The phase transition from the liquid-expanded to the liquid-condensed state was also affected: Two phase transitions were detected, the first at a surface pressure of 13.4 mN/m and at a mean molecular area of 95.8 Å^2, and the second at a surface pressure of 30.6 mN/m and at an area of 60.4 Å^2. This suggests that a reorganization of the protein in the monolayer takes place during the compression. Unexpectedly, the presence of lysozyme did also affect the DDA monolayer, but to a lesser extent (Fig. 6A). The shape of the isotherm was unaltered (phase transition and collapse point), but overall the isotherm shifted towards a higher surface pressure.

The initial surface pressure of the DSPC monolayer was affected neither by α-lactalbumin nor by lysozyme (Fig. 6B). However, the presence of both proteins resulted in a more expanded isotherm for DSPC, which was evident by a shift to a larger surface pressure and a higher area per molecule before the proteins were squeezed out of the monolayer at a molecular area of approximately 50 Å^2. In the presence of α-lactalbumin, one phase transition was introduced at a surface pressure of 22.8 mN/m and a molecular area of 62.4 Å^2. For lysozyme, two phase transitions could be detected, the first one at a surface pressure of 23.5 mN/m and at an area of 58.7 Å^2, whereas the second occurred at a surface pressure of 35.4 mN/m and at an area of 49.5 Å^2 indicating a reorganization of the protein during the compression.

The maximum of the compression modulus reflects the elasticity and the packing efficiency of the monolayer [37,38]. Monolayers of DDA and DSPC showed maximum values for the compression moduli at 199 and 276 mN/m (Fig. 7 and Table 6), respectively, which are characteristic values for liquid-condensed phases (condensed films) corresponding to lipids in the gel state [38,39]. Both proteins reduced the maximum of the compressibility modulus of the DDA monolayer, as compared to the pure monolayer (103 and 122 mN/m, respectively) suggesting a more liquid and flexible film [38,39]. The maximum of Cs^{-1} appeared at the same surface pressure (approximately 30 mN/m) for pure DDA and for DDA with lysozyme, but shifted towards a higher surface pressure in the presence of α-lactalbumin, indicating a late and maybe incomplete squeeze out of the protein. In contrast, no change could be observed for the DSPC monolayer, and the film packing was unaltered at high surface pressure due to a complete squeeze out of both proteins (Fig. 7B).

4. Discussion

Proteins can interact with liposomes in various ways, including i) binding to the polar lipid headgroups, ii) partial penetration into the hydrophobic membrane core, and iii) full permeation of the membrane bilayer [40]. These interactions are orchestrated via a number of different driving forces, i.e. electrostatic interactions, van der Waals forces and hydrophobic interactions, and the sum of these forces determines the nature of the interaction.

It has previously been shown that α-lactalbumin binds to negatively charged membranes at pH values below or close to the pI of the protein [41,42]. Below the pI, α-lactalbumin has a positive net charge, which favors attractive surface charge interactions with the anionic lipid headgroups [41,42]. A similar dependency on electrostatic attractions was evident in this study. At pH 7.4, the negatively charged α-lactalbumin interacted with the cationic liposomes, whereas no interactions could be measured between the positively charged lysozyme and the cationic liposomes, or between either of the proteins and the zwitterionic liposomes. This was evident from the "all or nothing" behavior observed for the size and zeta potential measurements and the DSC analyses, in which the electrostatic attraction appeared to be the driving force for the interactions.

Though the main interaction force in play appeared to be electrostatic attraction the results also pointed towards the existence of subsequent hydrophobic interactions. In fact, the cryo-TEM pictures clearly showed lipid fragments coated with α-lactalbumin (Fig. 2C), which suggests that membrane rearrangements and even disruption may take place upon protein binding implying the involvement of hydrophobic interactions. Furthermore, the range of protein-to-lipid molar ratios at which protein aggregation was induced (Fig. 1A), is rather large, as compared to studies in the literature with BSA and ovalbumin [17]. The upper ratio limit for aggregation was more than 100 times larger than the values previously measured for BSA and ovalbumin, which could indicate that the liposomal surface area available for protein adsorption becomes larger as the protein-to-lipid molar ratio increases due to membrane deformation and disruption. This phenomenon might eventually explain the membrane fragmentation observed by using cryo-TEM.

Table 5
The surface pressure of DSPC monolayers at minimum compression, at the collapse point and at the phase transitions, the two latter are also described by the mean molecular area. The results denote mean ± SD (n = 3).

	Minimum compression	Collapse point		Phase transition	
	mN/m	*mN/m*	*Å²*	*mN/m*	*Å²*
DSPC	0.2 ± 0.1	60.9 ± 0.8	42.2 ± 2.7	a	a
DSPC + α-lactalbumin	0.3 ± 0.1	62.4 ± 0.9	38.7 ± 0.5	22.8 ± 0.9	62.4 ± 0.3***
DSPC + lysozyme	0.1 ± 0.1	62.2 ± 1.7	39.0 ± 1.2	23.5 ± 1.4	58.7 ± 0.3
				35.4 ± 0.7***	49.5 ± 0.4

[a]No detectable phase transition.
*** $p < 0.0001$, as compared to DDA + lysozyme.

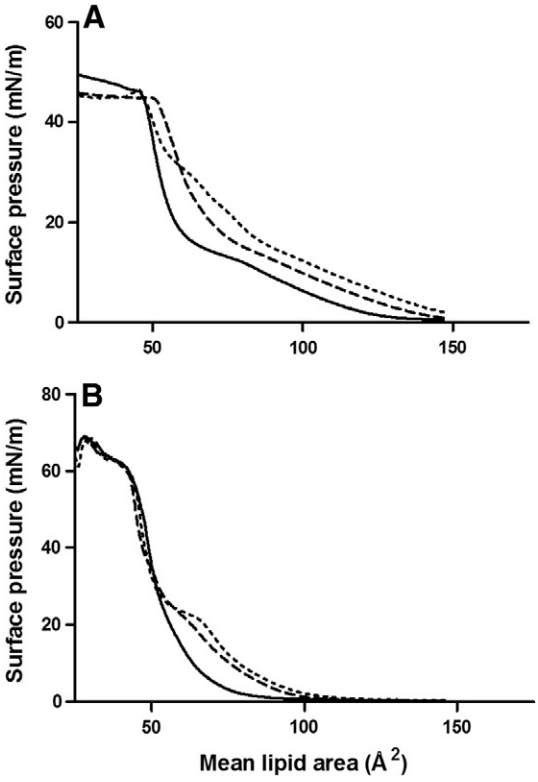

Fig. 6. Pressure/lipid area isotherms of Langmuir monolayers composed of A) DDA with 10 mM Tris buffer in the subphase (solid), 4.5 nmol α-lactalbumin in the subphase (dot) and 4.5 nmol lysozyme in the subphase (dash), B) DSPC with 10 mM Tris buffer in the subphase (solid), 4.5 nmol α-lactalbumin in the subphase (dot) and 4.5 nmol lysozyme in the subphase (dash). The curves represent averages of three experiments.

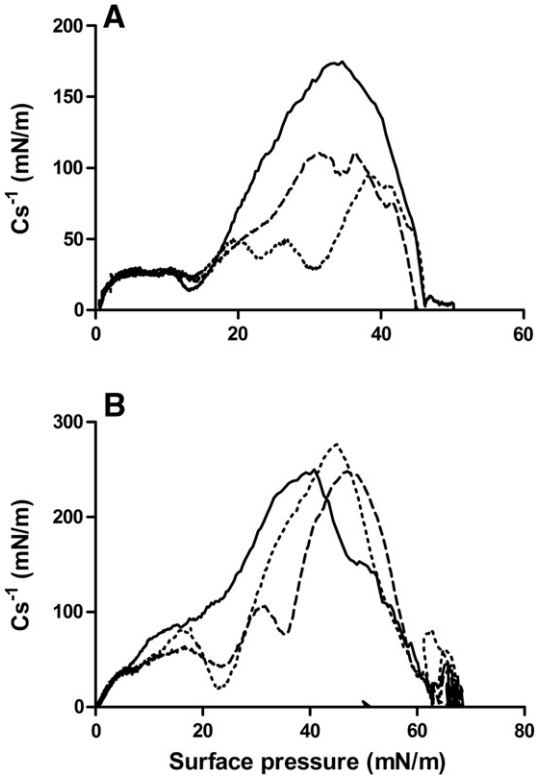

Fig. 7. Compression modulus derived from the pressure/area isotherms of the monolayers shown in Fig. 6. A) DDA with 10 mM Tris buffer in the subphase (solid), 4.5 nmol α-lactalbumin in the subphase (dot) and 4.5 nmol lysozyme in the subphase (dash), B) DSPC with mM Tris buffer in the subphase (solid), 4.5 nmol α-lactalbumin in the subphase (dot) and 4.5 nmol lysozyme in the subphase (dash). The curves represent averages of three experiments.

The involvement of hydrophobic interactions was also evident from the DSC studies showing that α-lactalbumin affected the packing of the lipids above the main phase transition temperature, and that the reversible nature of the thermotropic phase behavior was lost. Addition of α-lactalbumin to the ternary bilayer mixtures induced membrane rearrangements, eventually resulting in the formation of microdomains enriched in either DDA or DSPC in order to match the charge density on the surface of α-lactalbumin [43,44]. During the second scan, the peak resulting from the DDA domains was diminished, while the peak resulting from the DSPC domains remained unchanged. These results indicate that α-lactalbumin upon binding to the cationic headgroups of DDA interacts with the hydrophobic membrane interior of the cationic DDA liposomes, presumably both in the gel state and certainly in the liquid state when the fluidity of the membrane is increased.

The hydrophobic interaction may be the result of different interaction mechanisms and it might also be related to specific structural characteristics of α-lactalbumin. Halskau et al. proposed a model for the interaction between negatively charged phospholipid membranes and α-lactalbumin, and suggested that the interaction is initiated by the establishment of electrostatic attractions, followed by a loosening of α-lactalbumin's tertiary structure. This causes the exposure of hydrophobic areas of the protein, which then intercalate into the bilayer, eventually leading to membrane disruption [41,45]. However, deformations and disruption of cationic liposomes have also been reported to be a result of the ionic strength of the suspension medium, which causes fusion [46,47], or a result of the existence of a hyperosmotic gradient across the membrane, which deflates the liposomes and causes coalescence [48]. Accordingly, several stress factors might thus be responsible for the membrane disruption.

The Langmuir isotherms were used to further elucidate the hydrophobic interactions. Both α-lactalbumin and lysozyme are surface-active proteins that partially unfold at the air–water interface increasing their apparent hydrophobic surface area [34]. Hence, hydrophobic interactions are expected. The isotherm of the DSPC monolayer showed that the initial surface pressure of the DSPC monolayer was unaffected by the presence of both α-lactalbumin and lysozyme. However, the addition of both proteins to the subphase resulted in a more expanded isotherm for DSPC, measured as a shift towards a higher surface pressure and a higher area per molecule before they were completely squeezed out of the monolayer. This indicates that the proteins engage in hydrophobic interactions with the apolar lipid tails, which stretch over the proteins creating tilt deformations [35,36]. Once the lateral pressure exceeds a certain "exclusion pressure" the proteins are squeezed out into the sub phase [31]. The almost complete squeeze out was also evident from the compression moduli, which indicates that the packing of the lipid tails in the condensed state is unaffected by the presence of the proteins.

On the other hand, the proteins were not completely squeezed out of the DDA monolayer, most likely because the interactions are based on a

Table 6
The maximum compression modulus. The results denote mean ± SD (n = 3).

	Maximum Cs^{-1}
	mN/m
DDA	199 ± 30
DDA + α-lactalbumin	103 ± 7**
DDA + lysozyme	122 ± 10**
DSPC	276 ± 23
DSPC + α-lactalbumin	283 ± 24
DSPC + lysozyme	276 ± 22

** $p < 0.01$, as compared to DDA.

combination of hydrophobic and electrostatic interactions. This might suggest that a certain distribution of charged/hydrophobic patches is needed to enable the simultaneous hydrophobic and electrostatic interactions. The incomplete squeeze out was also evident from the reduced compression moduli in the presence of each protein, indicating the existence of a less ordered monolayer state than the liquid condensed phase [38,39]. It is unexpected that the net positively charged lysozyme is not completely squeezed out due to the overall electrostatic repulsion. Instead, the incomplete squeeze out observed for lysozyme is likely to be a consequence of the local distribution of the hydrophobic and the negatively charged domains in the protein.

In the Langmuir set-up, the exposure to the air–water interface partially results in the unfolding of the proteins at the interface [34], and this specific condition as such is not representative for the interfacial conditions in a dispersion of liposomes and proteins. Nonetheless, the intrinsic fluorescence studies showed that α-lactalbumin was significantly unfolded upon adsorption. The tertiary structure was loosened, the protein showed increased flexibility, and the hydrophobic entities, which are otherwise buried in the native protein, are exposed upon adsorption to the DDA/TDB liposomes, possibly due to the disruption of the Ca^{2+}-binding loop [26]. In the Langmuir setup, the unfolding of the proteins occurred before the compression, providing the possibility for insertion of the protein into the monolayer, as compared to the interaction with liposomes, where the membrane is tightly packed initially. Nonetheless, the Langmuir studies clearly demonstrate how the concerted action of the electrostatic and hydrophobic forces co-exists and stresses the membrane packing, and this could thus explain the disruption of the liposomes in the gel state (Fig. 8).

The present study illustrates that interaction between protein/peptide-based antigens and liposome-based adjuvants/vaccine delivery systems can markedly affect vaccine stability and the way these antigens are presented. This may have an important influence on the ability of the vaccine to induce the required immune responses. The present study thus emphasizes the importance of investigating the interaction between antigen and adjuvant for each novel vaccine tested in order to ensure optimal stability and immunogenicity.

5. Conclusions

The present study clearly demonstrates that the complex nature of subunit vaccine formulations, which are composed of both low-concentration protein antigen(s) and (particulate) adjuvants, necessitates the combined use of a number of biophysical methods for the physicochemical characterization. The interactions between protein antigens and CAF01/NAF01 were shown to be dominated by electrostatic interactions by applying methods like dynamic light scattering and cryoTEM. However, hydrophobic interactions did also play a role for the interaction, which was particularly evident from the DSC data and the Langmuir studies that provided important mechanistic information about the interfacial properties of the proteins and the membranes. α-Lactalbumin has some specific structural characteristics (size, hydrophobic pattern and flexibility) that might favor hydrophobic interactions with CAF01 which in this case affected both the type of adjuvant association as well as the structural integrity.

Further studies are needed to investigate the generality of these phenomena, including clinically relevant and more complex protein antigens, and to relate them to the immunogenicity of the antigens. Such studies might be important early in the development phase to predict interactions that lead to destabilizing stresses upon mixing and adsorption during processing and manufacture.

Notes

The authors declare no competing financial interest.

Acknowledgements

We acknowledge Gunnel Karlsson (Lund University) for performing the Cryo-TEM analysis. The work was funded by the Faculty of Health and Medical Sciences, University of Copenhagen, Denmark (MH), The Danish National Advanced Technology Foundation (grant numbers 007-2007-1 and 069-2011-1) and the Danish Strategic Research Council (grant number 09-067052). We acknowledge the Danish Agency for

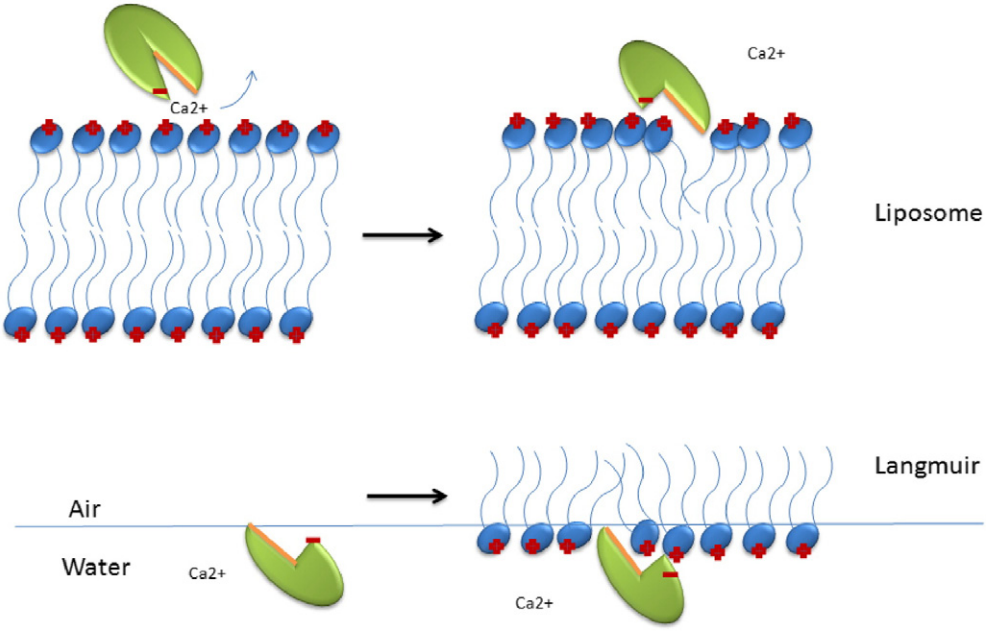

Fig. 8. Graphical illustration of the interactions between α-lactalbumin and cationic lipid-based Langmuir monolayers or liposome bilayers, respectively. For the liposomes, the interaction with α-lactalbumin is initiated by the establishment of electrostatic attractions. Subsequently, Ca^{2+} is released upon adsorption to the cationic lipid, followed by a loosening of the tertiary protein structure. The result is the exposure of hydrophobic areas of the protein, which then intercalate into the bilayer leading to membrane disruption. For the Langmuir monolayers, the exposure to the air–water interface causes α-lactalbumin to partially unfold prior to the spreading of the lipids on the subphase. Upon compression, α-lactalbumin is not squeezed out of the monolayer, which confirms the coexistence of electrostatic forces and strong hydrophobic interactions, which cause liposome disruption.

Science, Technology and Innovation for funding the Zetasizer Nano ZS and The Danish National Advanced Technology Foundation and the Danish Ministry of Science, Technology and Innovation for funding the nano-DSC and the ITC. The Drug Research Academy, University of Copenhagen, is kindly acknowledged for funding the NanoDrop and for co-funding the KSV Minitrough 1. We thank Apotekerfonden af 1991 for funding the Spex Fluorolog 3-22 fluorescence spectrometer. Finally, we acknowledge Novo Nordisk A/S for co-funding the VP-DSC MicroCalorimeter. The funding sources had no involvement in the study design; in the collection, analysis and interpretation of data; in the writing of the paper; or in the decision to submit the paper for publication.

Appendix A. Supplementary data

Thermograms and Langmuir monolayer isotherms of the proteins are available as Supporting information. The thermodynamic parameters for the proteins and the protein–liposome mixtures are also available as Supporting information. Supplementary data to this article can be found online at http://dx.doi.org/10.1016/j.bbamem.2014.04.013.

Appendix A. Supplementary data

Supplementary data to this article can be found online at http://dx.doi.org/10.1016/j.bbamem.2014.04.013.

References

[1] R. Rappuoli, Reverse vaccinology, Curr. Opin. Microbiol. 3 (2000) 445–450.
[2] R. Rappuoli, C.W. Mandl, S. Black, E. De Gregorio, Vaccines for the twenty-first century society, Nat. Rev. Immunol. 11 (2011) 865–872.
[3] J.H. Wilson-Welder, M.P. Torres, M.J. Kipper, S.K. Mallapragada, M.J. Wannemuehler, B. Narasimhan, Vaccine adjuvants: current challenges and future approaches, J. Pharm. Sci. 98 (2009) 1278–1316.
[4] R. Rappuoli, Bridging the knowledge gaps in vaccine design, Nat. Biotechnol. 25 (2007) 1361–1366.
[5] J.W. Yoo, D.J. Irvine, D.E. Discher, S. Mitragotri, Bio-inspired, bioengineered and biomimetic drug delivery carriers, Nat. Rev. Drug Discov. 10 (2011) 521–535.
[6] J. Davidsen, I. Rosenkrands, D. Christensen, A. Vangala, D. Kirby, Y. Perrie, E.M. Agger, P. Andersen, Characterization of cationic liposomes based on dimethyldioctadecylammonium and synthetic cord factor from *M. tuberculosis* (trehalose 6,6′-dibehenate)—a novel adjuvant inducing both strong CMI and antibody responses, Biochim. Biophys. Acta 1718 (2005) 22–31.
[7] M. Henriksen-Lacey, V.W. Bramwell, D. Christensen, E.M. Agger, P. Andersen, Y. Perrie, Liposomes based on dimethyldioctadecylammonium promote a depot effect and enhance immunogenicity of soluble antigen, J. Control. Release 142 (2009) 180–186.
[8] A.T. Kamath, B. Mastelic, D. Christensen, A.F. Rochat, E.M. Agger, D.D. Pinschewer, P. Andersen, P.H. Lambert, C.A. Siegrist, Synchronization of dendritic cell activation and antigen exposure is required for the induction of Th1/Th17 responses, J. Immunol. 188 (2012) 4828–4837.
[9] I.F. Matsunaga, D.B. Moody, Mincle is a long sought receptor for mycobacterial cord factor, J. Exp. Med. 206 (2009) 2865–2868.
[10] D. Christensen, M. Henriksen-Lacey, A.T. Kamath, T. Lindenstrom, K.S. Korsholm, J.P. Christensen, A.F. Rochat, P.H. Lambert, P. Andersen, C.A. Siegrist, Y. Perrie, E.M. Agger, A cationic vaccine adjuvant based on a saturated quaternary ammonium lipid have different in vivo distribution kinetics and display a distinct CD4 T cell-inducing capacity compared to its unsaturated analog, J. Control. Release 160 (2012) 468–476.
[11] M. Henriksen-Lacey, D. Christensen, V.W. Bramwell, T. Lindenstrom, E.M. Agger, P. Andersen, Y. Perrie, Liposomal cationic charge and antigen adsorption are important properties for the efficient deposition of antigen at the injection site and ability of the vaccine to induce a CMI response, J. Control. Release 145 (2010) 102–108.
[12] M. Henriksen-Lacey, A. Devitt, Y. Perrie, The vesicle size of DDA:TDB liposomal adjuvants plays a role in the cell-mediated immune response but has no significant effect on antibody production, J. Control. Release 154 (2011) 131–137.
[13] A. Joseph, N. Itskovitz-Cooper, S. Samira, O. Flasterstein, H. Eliyahu, D. Simberg, I. Goldwaser, Y. Barenholz, E. Kedar, A new intranasal influenza vaccine based on a novel polycationic lipid – ceramide carbamoyl-spermine (CCS) – I. Immunogenicity and efficacy studies in mice, Vaccine 24 (2006) 3990–4006.
[14] Y. Perrie, P.M. Frederik, G. Gregoriadis, Liposome-mediated DNA vaccination: the effect of vesicle composition, Vaccine 19 (2001) 3301–3310.
[15] M. Henriksen-Lacey, K.S. Korsholm, P. Andersen, Y. Perrie, D. Christensen, Liposomal vaccine delivery systems, Expert Opin. Drug Deliv. 8 (2011) 505–519.
[16] L.R. Tsuruta, W. Quintilio, M.H. Costa, A.M. Carmona-Ribeiro, Interactions between cationic liposomes and an antigenic protein: the physical chemistry of the immunoadjuvant action, J. Lipid Res. 38 (1997) 2003–2011.
[17] M. Hamborg, L. Jorgensen, A.R. Bojsen, D. Christensen, C. Foged, Protein antigen adsorption to the DDA/TDB liposomal adjuvant: effect on protein structure, stability, and liposome physicochemical characteristics, Pharm. Res. 30 (2012) 140–155.
[18] C.C. Bigelow, On the average hydrophobicity of proteins and relation between it and protein structure, J. Theor. Biol. 16 (1967) 187–211.
[19] E. Keshavarz, S. Nakai, Relationship between hydrophobicity and interfacial-tension of proteins, Biochim. Biophys. Acta 576 (1979) 269–279.
[20] K.R. Acharya, D.I. Stuart, N.P.C. Walker, M. Lewis, D.C. Phillips, Refined structure of baboon alpha-lactalbumin at 1.7-A resolution — comparison with C-type lysozyme, J. Mol. Biol. 208 (1989) 99–127.
[21] C.C.F. Blake, D.F. Koenig, G.A. Mair, A.C.T. North, D.C. Phillips, V.R. Sarma, Structure of hen egg-white lysozyme — a 3-dimensional fourier synthesis at 2 A resolution, Nature 206 (1965) 757–761.
[22] D. Christensen, D. Kirby, C. Foged, E.M. Agger, P. Andersen, Y. Perrie, H.M. Nielsen, Alpha,alpha′-trehalose 6,6′-dibehenate in non-phospholipid-based liposomes enables direct interaction with trehalose, offering stability during freeze-drying, Biochim. Biophys. Acta 1778 (2008) 1365–1373.
[23] K. Brew, T.C. Vanaman, R.L. Hill, Comparison of amino acid sequence of bovine alpha-lactalbumin and hens egg white lysozyme, J. Biol. Chem. 242 (1967) 3747–3748.
[24] W.J. Browne, A.C.T. North, D.C. Phillips, A possible 3-dimensional structure of bovine alpha-lactalbumin based on that of hens egg-white lysozyme, J. Mol. Biol. 42 (1969) 65–86.
[25] D.I. Stuart, K.R. Acharya, N.P.C. Walker, S.G. Smith, M. Lewis, D.C. Phillips, Alpha-lactalbumin possesses a novel calcium-binding loop, Nature 324 (1986) 84–87.
[26] E.D. Chrysina, K. Brew, K.R. Acharya, Crystal structures of apo- and holo-bovine alpha-lactalbumin at 2.2-A resolution reveal an effect of calcium on inter-lobe interactions, J. Biol. Chem. 275 (2000) 37021–37029.
[27] K. Kuwajima, The molten globule state of alpha-lactalbumin, FASEB J. 10 (1996) 102–109.
[28] D. Chaudhuri, M. Narayan, L.J. Berliner, Conformation-dependent interaction of alpha-lactalbumin with model and biological membranes: a spin-label ESR study, Protein J. 23 (2004) 95–101.
[29] M.J. Kronman, L.G. Holmes, Inter- and intramolecular interactions of alpha-lactalbumin. 4. Location of tryptophan groups, Biochemistry 4 (1965) 526–532.
[30] W.R. Glomm, S. Volden, O. Halskau, M.H.G. Ese, Same system-different results: the importance of protein. Introduction protocols in Langmuir-monolayer studies of lipid–protein interactions, Anal. Chem. 81 (2009) 3042–3050.
[31] P. Toimil, G. Prieto, J. Minones, J.M. Trillo, F. Sarmiento, Interaction of human serum albumin with monofluorinated phospholipid monolayers, J. Colloid Interface Sci. 388 (2012) 162–169.
[32] D. Marsh, Lateral pressure in membranes, Biochim. Biophys. Acta Rev. Biomembr. 1286 (1996) 183–223.
[33] D.R. Shnek, D.W. Pack, D.Y. Sasaki, F.H. Arnold, Specific protein attachment to artificial membranes via coordination to lipid-bound copper(II), Langmuir 10 (1994) 2382–2388.
[34] I. Langmuir, V.J. Schaefer, Properties and structure of protein monolayers, Chem. Rev. 24 (1939) 181–202.
[35] S. May, A. Ben-Shaul, Molecular theory of lipid–protein interaction and the L-alpha-H-II transition, Biophys. J. 76 (1999) 751–767.
[36] S. May, Y. Kozlovsky, A. Ben-Shaul, M.M. Kozlov, Tilt modulus of a lipid monolayer, Eur. Phys. J. E 14 (2004) 299–308.
[37] D. Vollhardt, V.B. Fainerman, Progress in characterization of Langmuir monolayers by consideration of compressibility, Adv. Colloid Interf. Sci. 127 (2006) 83–97.
[38] J.T. Davies, E.K. Rideal, Properties of Monolayers, Interfacial Phenomena, Academic Press Inc., New York, 1961. 217–279.
[39] M. Kepczynski, J. Lewandowska, K. Witkowska, S. Kedracka-Krok, V. Mistrikova, J. Bednar, P. Wydro, M. Nowakowska, Bilayer structures in dioctadecyldimethylammonium bromide/oleic acid dispersions, Chem. Phys. Lipids 164 (2011) 359–367.
[40] D. Papahadjopoulos, M. Moscarello, E.H. Eylar, T. Isac, Effects of proteins on thermotropic phase transitions of phospholipid membranes, Biochim. Biophys. Acta 401 (1975) 317–335.
[41] O. Halskau, N.A. Froystein, A. Muga, A. Martinez, The membrane-bound conformation of alpha-lactalbumin studied by NMR-monitored H-1 exchange, J. Mol. Biol. 321 (2002) 99–110.
[42] A.V. Agasoster, O. Halskau, E. Fuglebakk, N.A. Froystein, A. Muga, H. Holmsen, A. Martinez, The interaction of peripheral proteins and membranes studied with alpha-lactalbumin and phospholipid bilayers of various compositions, J. Biol. Chem. 278 (2003) 21790–21797.
[43] D. Harries, S. May, A. Ben-Shaul, Adsorption of charged macromolecules on mixed fluid membranes, Colloids Surf. A Physicochem. Eng. Asp. 208 (2002) 41–50.
[44] S. May, A. Ben-Shaul, A molecular model for lipid-mediated interaction between proteins in membranes, Phys. Chem. Chem. Phys. 2 (2000) 4494–4502.
[45] I. Rodland, O. Halskau, A. Martinez, H. Holmsen, Alpha-lactalbumin binding and membrane integrity — effect of charge and degree of unsaturation of glycerophospholipids, Biochim. Biophys. Acta Biomembr. 1717 (2005) 11–20.
[46] L.A.M. Rupert, D. Hoekstra, J.B.F.N. Engberts, Fusogenic behavior of didodecyldimethylammonium bromide bilayer vesicles, J. Am. Chem. Soc. 107 (1985) 2628–2631.
[47] A.M. Carmona-Ribeiro, H. Chaimovich, Salt-induced aggregation and fusion of dioctadecyldimethylammonium chloride and sodium dihexadecylphosphate vesicles, Biophys. J. 50 (1986) 621–628.
[48] P. Saveyn, J. Cocquyt, P. Bomans, P. Frederik, M. De Cuyper, P. Van der Meeren, Osmotically induced morphological changes of extruded dioctadecyldimethylammonium chloride (DODAC) dispersions, Langmuir 23 (2007) 4775–4781.